

## Lattice dynamics of zinc-blende GaN and AlN: I. Bulk phonons

This article has been downloaded from IOPscience. Please scroll down to see the full text article.

1996 J. Phys.: Condens. Matter 8 6323

(<http://iopscience.iop.org/0953-8984/8/35/003>)

View [the table of contents for this issue](#), or go to the [journal homepage](#) for more

Download details:

IP Address: 171.66.16.206

The article was downloaded on 13/05/2010 at 18:34

Please note that [terms and conditions apply](#).

# Lattice dynamics of zinc-blende GaN and AlN: I. Bulk phonons

Jian Zi†, Xin Wan, Guanghong Wei, Kaiming Zhang and Xide Xie

Fudan–T D Lee Physics Laboratory and Surface Physics Laboratory, Fudan University, Shanghai 200433, People's Republic of China

Received 3 January 1996, in final form 24 June 1996

**Abstract.** The lattice dynamics of zinc-blende GaN and AlN were studied theoretically using a two-parameter Keating potential together with the long-range Coulomb interactions. Phonon frequencies transformed from those of the wurtzite counterparts were used to determine the two Keating parameters and the effective charge. We present for the first time the phonon dispersion curves for zinc-blende GaN and AlN. An interesting feature was found for the phonons propagating along the [110] direction, which does not exist in other III–V semiconductors.

## 1. Introduction

Gallium nitride (GaN) and aluminium nitride (AlN) are two of the most promising III–V semiconductors for short-wavelength optoelectronic devices. They have received considerable research interest [1]. In the past several years, much notable progress has been made with III–V nitrides. Recently, an efficient blue-light-emitting diode has been achieved using Si-doped GaN [2]. At present, semiconductor optical devices routinely operate from the IR to green wavelengths. If the range could be extended into the blue wavelengths, the three primary colour semiconductor diodes could be obtained, which would have a great impact on imaging and graphics applications. Like most other wide band-gap semiconductors, the nitrides exhibit superior radiation hardness compared with GaAs and Si, which also makes them attractive for space applications. Under ambient conditions, GaN and AlN have the hexagonal wurtzite structure. Although GaN and AlN are well-known to be highly stable in the wurtzite structures, zinc-blende GaN has been experimentally observed [3]: it is expected that zinc-blende GaN is more amenable to doping than wurtzite GaN, since all of the III–V semiconductors that can be efficiently doped (n-type or p-type) are cubic. Therefore, it is meaningful to characterize both experimentally and theoretically the physical properties of zinc-blende III–V nitrides.

There have been many theoretical studies on the electronic properties of both wurtzite and zinc-blende GaN and AlN [1]. Raman spectroscopy, which detects phonon frequencies near the zone centre, has been adopted to study the vibrational properties of wurtzite GaN [4, 5, 6, 7, 8, 9, 10] and AlN [11]. To our knowledge, no experimental phonon dispersion curves for GaN and AlN have been reported so far due to the difficulty in obtaining high-quality samples. On the theoretical side, only the TO phonon frequencies at the zone centre for zinc-blende GaN and AlN were obtained by a first-principles pseudopotential calculation

† Electronic address: jianzi@fudan.ihep.ac.cn

[12] and by a full-potential linear muffin-tin orbital method [13]. In the present work, we try to give the phonon dispersion curves for zinc-blende GaN and AlN theoretically.

The paper is organized as follows. In section 2 the model used and calculation method are briefly described. Section 3 gives the calculated results and some discussions.

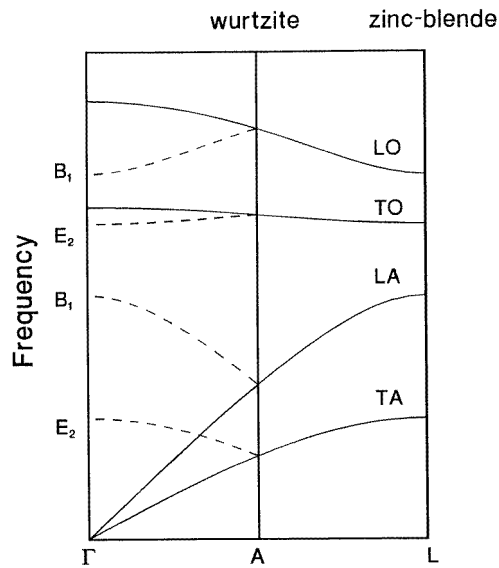


**Figure 1.** Phonon dispersion relations of the zinc-blende structure for phonon propagating along the  $\Gamma$ -L ([111]) direction and of the wurtzite structure for phonons propagating along the  $\Gamma$ -A ([0001]) direction.

## 2. Theoretical models

A two-parameter Keating potential [14] and the long-range Coulomb interaction between ions were considered in the present work. The short-range Keating potential involves the bonding-stretching and bond-bending interactions. The bonding-stretching term is a two-body interaction given by

$$\frac{2}{a^2} \sum_{s,s'} \alpha (\mathbf{R}_{ss'} \cdot \mathbf{R}_{ss'} - r_0^2)^2 \quad (1)$$

and the bond-bending term is a three-body interaction

$$\frac{2}{a^2} \sum_{s,s' \neq s''} \beta (\mathbf{R}_{ss'} \cdot \mathbf{R}_{ss''} + \frac{1}{3} r_0^2)^2 \quad (2)$$

where  $a$  is the lattice constant and  $r_0$  the equilibrium bond length;  $s'$  and  $s''$  are the neighbouring atoms bonding to the atom  $s$  and  $\mathbf{R}_{ss'} = \mathbf{R}_s - \mathbf{R}_{s'}$  stands for the relative position vector between two atoms which form a bond. The parameters  $\alpha$  and  $\beta$  describe the bond-stretching and bond-bending interactions, respectively. This model has been widely used to study elastic [14, 15] and structural [16, 17, 18] properties of covalent crystals. It also has been successfully used to describe the lattice dynamics of semiconductors [19] and semiconductor superlattices [20, 21, 22].

The long-range interaction is assumed to have the Coulomb form

$$\frac{Z_i Z_j e^2}{R_{ij}} \quad (3)$$

where  $R_{ij}$  is the distance between the atoms  $i$  and  $j$  and  $Z_i, Z_j = \pm Z_{\text{eff}}$  with  $Z_{\text{eff}}$  being the effective charge. Hence, there are three parameters involved in the present model: two Keating parameters  $\alpha$  and  $\beta$ , and the effective charge  $Z_{\text{eff}}$ .

**Table 1.** Corresponding phonon modes in the wurtzite and zinc-blende structures and the experimental data.

Wurtzite mode	Zinc-blende mode	GaN <sup>a</sup> (cm <sup>-1</sup> )	AlN <sup>b</sup> (cm <sup>-1</sup> )
$E_2^{(1)}$	TA(L)	144	252
$E_2^{(2)}$	TO(L)	569	660
$\frac{1}{3}[A_1(\text{TO})+2E_1(\text{TO})]$	TO( $\Gamma$ )	552	653
$\frac{1}{3}[A_1(\text{LO})+2E_1(\text{LO})]$	LO( $\Gamma$ )	740	908

<sup>a</sup> Reference [10].

<sup>b</sup> Results of McNeil given in [11].

### 3. Results and discussions

The close relations between zinc-blende and wurtzite structures have long been recognized. The difference in the neighbouring atoms begins only in the third shell. Zinc-blende crystals are cubic with two atoms per unit cell, whereas wurtzite crystals are hexagonal with four atoms per unit cell. Therefore, the Brillouin zone of zinc-blende along the [111] direction is twice as large as that of the wurtzite along the [0001] direction. Hence, one could derive the phonon dispersions for the wurtzite structures by simply folding the ones for the zinc-blende structures [23] as shown in figure 1. The two non-polar modes  $E_2$  in the wurtzite structure correspond to the TO(L) and TA(L) modes in the zinc-blende structure and the two non-polar  $B_1$  modes in the wurtzite correspond to the LO(L) and LA(L) modes in the zinc-blende. Owing to the macroscopic electric field induced by LO phonons the LO modes at the zone centre in zinc-blende split into  $A_1(\text{LO})$  and  $E_1(\text{LO})$  modes in the wurtzite structure and the same is true for TO modes. Therefore, the following correspondence is assumed accordingly

$$\text{LO}(\Gamma) \leftrightarrow \frac{1}{3} [A_1(\text{LO}) + 2E_1(\text{LO})] \quad (4)$$

$$\text{TO}(\Gamma) \leftrightarrow \frac{1}{3} [A_1(\text{TO}) + 2E_1(\text{TO})] \quad (5)$$

where the left-hand side represents for the zinc-blende modes and the right-hand side represents the wurtzite modes.

There are no experimental phonon frequencies available so far for zinc-blende GaN and AlN. One could, however, use the folding procedure described above to obtain the data for the zinc-blende GaN and AlN. Table 1 shows the experimental data for wurtzite GaN and AlN and transformed data for zinc-blende structures.

The effective charge parameter  $Z_{\text{eff}}$  can be determined so as to reproduce the experimental splitting of the LO and TO phonon frequencies at the zone centre

$$Z_{\text{eff}}^2 = \frac{(\omega_{\text{LO}}^2 - \omega_{\text{TO}}^2) M_r \Omega}{4\pi e^2} \quad (6)$$

where  $\Omega$  is the unit cell volume and  $M_r$  the reduced mass of the cation and anion atoms.

The bond-stretching and bond-bending parameters  $\alpha$  and  $\beta$  were obtained by fitting them to the values listed in table 1. The resulting Keating parameters  $\alpha$ ,  $\beta$ , and the effective charge  $Z_{\text{eff}}$  together with other data used in our calculations are given in table 2. It is found that the effective charge parameter  $Z_{\text{eff}}$  for both nitrides is much larger than that for arsenides and antimonides, which indicates the stronger ionic character of GaN and AlN.

**Table 2.** Parameters used for the calculations of phonon dispersions. The masses of cations and anions are denoted by  $m_c$  and  $m_a$ , respectively.  $\alpha$  and  $\beta$  are the Keating parameters.  $Z_{\text{eff}}$  is the effective charge parameter and  $a$  is the lattice constant.

	$m_c$	$m_a$	$\alpha$ (Nm <sup>-1</sup> )	$\beta$ (Nm <sup>-1</sup> )	$Z_{\text{eff}}$	$a$ (Å)
GaN	69.72	14.01	66.48	1.59	1.147	4.5 <sup>a</sup>
AlN	26.98	14.01	75.15	3.72	1.269	4.421 <sup>b</sup>

<sup>a</sup> Data for epitaxially grown cubic GaN [24].

<sup>b</sup> Reference [12].

**Table 3.** The calculated phonon frequencies at the high-symmetry points in units of cm<sup>-1</sup>. The values in parentheses are the transformed data listed in table 1.

	TA	LA	TO	LO	
GaN	Γ		562(552)	748 (740)	
	X	207	286	558	639
	L	140 (144)	296	554 (569)	675
AlN	Γ		670 (653)	920 (908)	
	X	368	505	614	701
	L	244 (252)	501	638 (660)	761

With the obtained parameters one can construct the dynamical matrix. By solving the secular equation about the dynamical matrix the eigenfrequencies can be obtained. The contribution of the long-range Coulomb interaction to the force constants was calculated exactly by using the conventional Ewald method [25]. The calculated phonon frequencies at the high-symmetry points are given in table 3. It can be seen that the calculated results are in good agreement with the transformed experimental data. The calculated TO phonon frequency for zinc-blende GaN at the zone centre is 603 cm<sup>-1</sup> by the full-potential linear muffin-tin orbital method [13] and 558 cm<sup>-1</sup> by the *ab initio* pseudopotential calculations [12]. Our results agree well with those of the *ab initio* pseudopotential calculations. For zinc-blende AlN the calculated TO phonon frequency at the zone centre is 648 cm<sup>-1</sup> by the *ab initio* pseudopotential calculations, which is in reasonable agreement with our results.

Figures 2 and 3 show the calculated phonon dispersion curves for zinc-blende GaN and AlN along the [100], [110] and [111] directions. It can be seen from the figures that the TO mode in GaN is rather flat throughout the Brillouin zone. For phonons propagating along the [110] direction there is an interesting feature: the anti-crossing of two acoustic  $\Sigma_1$  branches. Because the two  $\Sigma_1$  modes belong to the same representation, strong intermixing occurs when they approach in the vicinity of the K point. As a result, they do not really cross. By a careful analysis, it is found that this feature is related to the relatively large effective charge of GaN and AlN under the present parametrization. It is quite obvious for

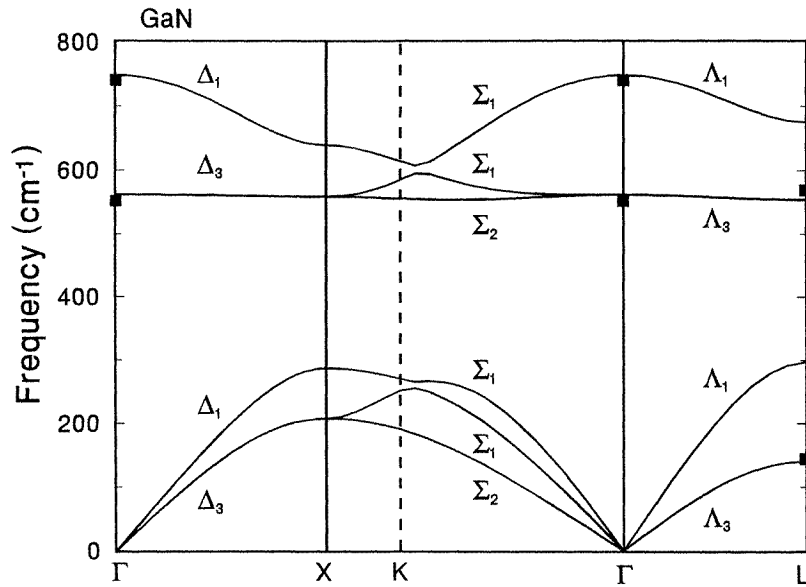


**Figure 2.** Calculated phonon dispersion curves (solid lines) for zinc-blende GaN. The transformed experimental data are marked by solid squares.

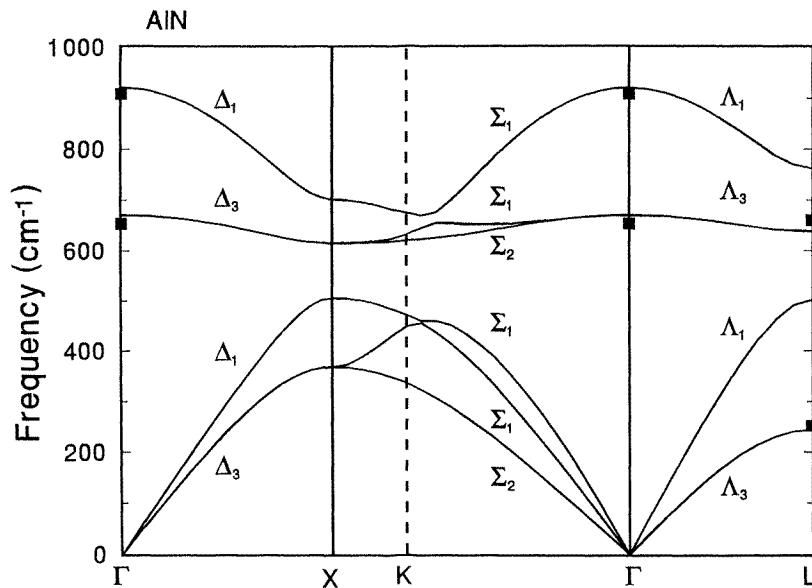


**Figure 3.** Calculated phonon dispersion curves (solid lines) for zinc-blende AlN. The transformed experimental data are marked by solid squares.

GaN. For AlN the two  $\Sigma_1$  branches do not really cross although it is hard to see from the figure. This feature occurs neither in Si, Ge, nor in other III-V semiconductors owing to

the fact that the two  $\Sigma_1$  branches are separated in the vicinity of the K point. However, in some semiconductors like SiC, there is also some small intermixing of the two acoustic  $\Sigma_1$  branches in the vicinity of the K point owing to the fact that the two branches are rather close [26]. As a result, the  $\Sigma_1$  branch with higher frequency exhibits a shoulder feature in the vicinity of the K point.

In conclusion, the phonon dispersion curves of zinc-blende GaN and AlN were studied by using the Keating potential for short-range interactions and the Coulomb potential for long-range interactions. Although there are no experimental Raman data available for zinc-blende nitrides, one could obtain them by a simple folding procedure of the data for wurtzite structures. The calculated results are in good agreement with the transformed data. An interesting feature, which does not exist in other III–V and IV semiconductors, was found for phonons propagating along the [110] direction.

### Acknowledgments

This work is supported in part by the Research Plan of Qi-Ming Star of Shanghai and the NSF of China.

### References

- [1] For a review see, for example,  
Strite S and Morkoç H 1992 *J. Vac. Sci. Technol. B* **10** 1237
- [2] Koide N, Kato H, Sassa M, Yamasaki S, Manabe K, Hashimoto M, Amano H, Hiramatsu K and Akasaki I 1991 *J. Cryst. Growth* **115** 639
- [3] Moustakas T D, Lei L and Molnar R J 1993 *Physica B* **185** 36
- [4] Manchon D D Jr, Barker A S Jr, Dean P J and Zetterstrom R B 1970 *Solid State Commun.* **8** 1227
- [5] Lemos V, Arguello C A and Leite R C C 1972 *Solid State Commun.* **11** 1351
- [6] Cingolani A, Ferrara M, Lugará M and Scamarcio G 1986 *Solid State Commun.* **58** 823
- [7] Kubota K, Kobayashi Y and Fujimoto K 1989 *J. Appl. Phys.* **66** 2984
- [8] Humphreys T P, Sukov C A, Nemanich R J, Posthill J B, Budder R A, Hattangady S V and Markunas R J 1990 *Mater. Res. Soc. Symp. Proc.* **162** 531
- [9] Hayashi K, Itoh K, Sawaki N and Akasaki I 1991 *Solid State Commun.* **77** 115
- [10] Azuhata T, Sota T, Suzuki K and Nakamura S 1995 *J. Phys.: Condens. Matter* **7** L129
- [11] Perlin P, Polian A and Suski T 1993 *Phys. Rev. B* **47** 2874
- [12] Miwa K and Fukumoto A 1993 *Phys. Rev. B* **48** 7879
- [13] Kim K, Lambrecht W R L and Segall B 1994 *Phys. Rev. B* **50** 1502
- [14] Keating P N 1966 *Phys. Rev.* **145** 637
- [15] Martin R M 1970 *Phys. Rev. B* **1** 4005
- [16] Pedersen J S 1989 *Surf. Sci.* **210** 238
- [17] Appelbaum J A and Hamann D R 1978 *Surf. Sci.* **74** 21
- [18] Tromp R M 1985 *Surf. Sci.* **155** 432
- [19] Baraff G A, Kane E O and Schluter M 1980 *Phys. Rev. B* **21** 5662
- [20] Zi Jian, Zhang Kaiming and Xie Xide 1990 *Phys. Rev. B* **41** 12862
- [21] Alonso M I, Cardona M and Kanellis G 1989 *Solid State Commun.* **69** 479
- [22] Lee I and Fong C Y 1991 *Phys. Rev. B* **44** 6270
- [23] Birman J L 1959 *Phys. Rev.* **115** 1493
- [24] Lei T, Moustakas T D, Graham R J, He Y and Berkowitz S J 1992 *J. Appl. Phys.* **71** 4933
- [25] Born M and Huang K 1956 *Dynamical Theory of Crystal Lattices* (Oxford: Oxford University Press)
- [26] Karch K, Pavone P, Windl W, Schütt C and Strauch D 1994 *Phys. Rev. B* **50** 17054